Qualitative analysis of the level of cross-protection between epidemic waves of the 1918–1919 influenza pandemic

D. Rios-Doria [a,*], G. Chowell [a,b]

[a] Mathematical, Computational and Modeling Sciences Center, School of Human Evolution and Social Change, Arizona State University, Tempe, AZ 85287, USA
[b] Division of Epidemiology and Population Studies, Fogarty International Center, National Institutes of Health, Bethesda, MD, USA

ABSTRACT

The 1918–1919 influenza pandemic was composed of multiple waves within a period of nine months in several regions of the world. Increasing our understanding of the mechanisms responsible for this multi-wave profile has important public health implications. We model the transmission dynamics of two strains of influenza interacting via cross-immunity to simulate two temporal waves of influenza and explore the impact of the basic reproduction number, as a measure of transmissibility associated to each influenza strain, cross-immunity and the timing of the onset of the second influenza epidemic on the pandemic profile. We use time series of case notifications during the 1918 influenza pandemic in Geneva, Switzerland, for illustration. We calibrate our mathematical model to the initial wave of infection to estimate the basic reproduction number of the first wave and the corresponding timing of onset of the second influenza variant. We use this information to explore the impact of cross-immunity levels on the dynamics of the second wave of influenza. Our results for the 1918 pandemic in Geneva, Switzerland, indicate that a second wave can occur whenever $R_{0_1} < 1.5$ or when cross-immunity levels are less than 0.58 for our estimated R_{0_2} of 2.4. We also explore qualitatively profiles of two-wave pandemics and compare them with real temporal profiles of the 1918 influenza pandemic in other regions of the world including several Scandinavian cities, New York City, England and Wales, and Sydney, Australia. Pandemic profiles are classified into three broad categories namely "right-handed", "left-handed", and "M-shape". Our results indicate that avoiding a second influenza epidemic is plausible given sufficient levels of cross-protection are attained via natural infection during an early (herald) wave of infection or vaccination campaigns prior to a second wave. Furthermore, interventions aimed at mitigating the first pandemic wave may be counterproductive by increasing the chances of a second wave of infection that could potentially be more virulent than the first.

© 2009 Elsevier Ltd. All rights reserved.

1. Introduction

The 1918–1919 influenza pandemic has been the most devastating of recent history in terms of morbidity and mortality burden with 20–100 million deaths worldwide (Patterson and Pyle, 1991) and significantly higher transmissibility compared to seasonal influenza epidemics (Chowell et al., 2006, 2008b). Moreover, two major waves of infection have been documented in various regions of the world for this pandemic during a relatively short period of time in between seasons (Chowell et al., 2006; Caley et al., 2007) with a reportedly higher case fatality rate for the second wave (Andreasen et al., 2008). Hence, increasing our theoretical understanding on the nature of the mechanisms responsible for the generation or elimination of

multiple pandemic waves could lead to better pandemic preparedness plans. Various studies have proposed several mechanisms for the generation of multiple waves during the 1918 influenza pandemic that include the impact of social distancing (Caley et al., 2007), the role of co-infection with acute respiratory infections (Merler et al., 2008) and behavior changes (Epstein et al., 2008). Multiple wave patterns could also be the result of the delayed introduction of the virus in different communities within the same region or even due to re-entry of the virus into the same community. In fact, the current pattern of the novel swine-origin influenza A (H1N1) virus (S-OIV) in Mexico follows a two wave profile with the first wave (April–May, 2009) affecting mostly the central region of the country and the second wave (June–July, 2009) focused in southern states (Mexico Ministry of Health, 2009). The role of interventions in a setting of multiple epidemic waves as a result of re-entry of the same infectious agent has been studied using a simple transmission model (Handel et al., 2007). Here we study the hypothesis that the

multiple epidemic waves in 1918 were due to the delayed circulation of two influenza strains that were not necessarily equally transmissible under different levels of cross-immunity. In the case of seasonal influenza, several experimental studies have documented the presence of cross-immunity in various communities (Taber et al., 1981; Fox et al., 1982). Recent work (Barry et al., 2008) has highlighted the role of cross-protective immunity acquired by individuals infected during the early spring/summer wave of the pandemic. This supports the idea that multiple waves in 1918 were due to closely related influenza variants. Barry et al. (2008) suggest that sequential variants of the A(H1N1) influenza virus could have been responsible for the multi-wave pattern of this unique pandemic. In fact, these researchers estimated that the first wave of the 1918 influenza pandemic yielded between 35% and 95% protection against reinfection for the second wave and between 56% and 89% protection against death using data from US Army training camps, the British Grand Fleet and British civilian communities (Barry et al., 2008). Hence, increasing population immunity levels during the early pandemic phase via natural infection and/or vaccination campaigns could avoid a second and potentially more lethal pandemic wave. We address this theoretical question via numerical simulations using as a framework a two-strain influenza transmission model. Our mathematical model accounts for cross-immunity between strains, the timing of onset of the second influenza variant strain into a partially susceptible population as well as the actual transmissibility associated to each influenza variant.

The dynamics of two strains of influenza introduced in sync into a completely susceptible population have been examined analytically (Dietz, 1979) and considered with various levels of cross-immunity (Castillo-Chavez et al., 1989; Nuño et al., 2005). However, no study has examined the role of varying the emergence time of a second strain and level of cross-immunity as a mechanism to explain multiple wave profiles. Here we use time series of case notifications during the 1918 influenza pandemic in Geneva, Switzerland, for illustration. We calibrate our mathematical model to the initial wave of infection to estimate the basic reproduction number of the first wave and the corresponding timing of onset of the second influenza epidemic. We use this information to explore the impact of cross-immunity on the second influenza wave and determine numerical threshold levels of cross-immunity for which the second wave of infection cannot occur. Furthermore, we also discuss the potential benefits of moderate levels of immunization with a vaccine of limited efficacy to reduce the likelihood of a second wave of infection. Finally, qualitative profiles of two-wave pandemics are simulated using our mathematical model and compared with real temporal profiles of the 1918 influenza pandemic from several regions of the world.

2. Materials and methods

2.1. The epidemic model

We developed an extension to an epidemic model previously calibrated to the spring and fall waves of the 1918 influenza pandemic in Geneva, Switzerland (Chowell et al., 2006). While the model in Chowell et al. (2006) was used to describe the summer and fall waves of the 1918–1919 pandemic, our extended model (Fig. 1) incorporates the dynamics of two influenza strains interacting via cross-immunity, see Dietz (1979), Castillo-Chavez et al. (1989) and Nuño et al. (2005). We assume that individuals recovered from one strain are completely protected against reinfection from the same strain but are susceptible to the other

circulating strain at a reduced level of susceptibility through a cross-immunity parameter. Furthermore, we assume the level of cross-immunity conferred to an individual is independent of the infection order of the two strains.

Our model classifies individuals as susceptible (S), exposed (E_i), clinically ill and infectious (I_i), asymptomatic and partially infectious (A_i), diagnosed (J_i) and recovered (R_i) where the index $i = 1, 2$ denotes each influenza strain. Cross-immunity is explored in terms of relative susceptibility (σ) to infection, where σ can be any value between zero and one ($\sigma \in [0, 1]$). Complete susceptibility to a variant strain (no cross-immunity) is given by $\sigma = 1$ while complete protection against a variant strain (full cross-immunity) is obtained when $\sigma = 0$. Similarly, a value of $\sigma = 0.10$ can be interpreted as 90% protection against infection to the second strain for individuals infected during the first wave by the first strain. Recovered individuals that are infected with a second strain may again become exposed (F_i), asymptomatic (Y_i), clinically infectious (V_i), diagnosed (H_i) and recovered (Z). We also keep track of the cumulative number of diagnosed cases, C.

For simplicity, we assume the population has the same birth and death rate (μ). That is, the average life expectancy of the population is given by $1/\mu$. Assuming a homogenous mixing population, susceptible individuals become infected when they come into contact with an infectious individual. The transmission rate of influenza is denoted by β_i. Latent individuals become infectious at rate κ_i. We define the proportion of clinical infections as ρ_i. Thus, the rate of exposed individuals progressing to the clinically infectious class I_i is $\kappa_i \rho_i$ while the remaining fraction progresses to the asymptomatic partially infectious class A_i at rate $\kappa_i(1 - \rho_i)$. Clinically infectious individuals recover at rate γ_{1_i} or are diagnosed at rate α_i. Diagnosed individuals recover at the adjusted rate $\gamma_{2,i} = 1/[1/\gamma_{1,i} - 1/\alpha_i]$ or die at the mortality rate which is adjusted based on the case fatality proportion (CFP), $\delta_i = [\text{CFP}_i/(1 - \text{CFP}_i)](\mu + \gamma_{2,i})$. The system of nonlinear differential equations governing the above transmission process is given in Appendix A.

When a single strain (initial strain, $i = 1$) is circulating in the population, the force of infection is a time dependent total rate of infection expressed as the product of the transmission rate β_i and the probability of coming into contact with an infectious individual. The force of infection is then given by $\beta_1(I_1(t) + J_1(t) + q_1 A_1(t))/N(t)$ where $N(t) = S(t) + E_1(t) + I_1(t) + A_1(t) + J_1(t) + R_1(t)$ and q_1 is the relative infectiousness of the asymptomatic class. Diagnosed individuals are assumed to be infectious due to the lack of evidence of effective interventions during the pandemic of 1918 (Ammon, 2001). When both strains are co-circulating the total population size is given by the summation of individuals in all classes,

$$N(t) = S(t) + Z(t)$$
$$+ \sum_{i=1}^{2} [E_i(t) + A_i(t) + I_i(t) + J_i(t) + R_i(t) + F_i(t) + Y_i(t) + V_i(t)$$
$$+ H_i(t)].$$

The force of infection for strain i in a population where both strains are co-circulating accounts for individuals infected by strain i as a secondary infection (after being infected by the other strain) and is given by

$$\lambda_i = \beta_i \frac{I_i(t) + J_i(t) + q_i A_i(t) + V_i(t) + H_i(t) + q_i Y_i(t)}{N(t)}$$

2.2. Data sources

Data for the 1918 influenza pandemic has been collected and reported reasonably well in various areas of the world. To calibrate
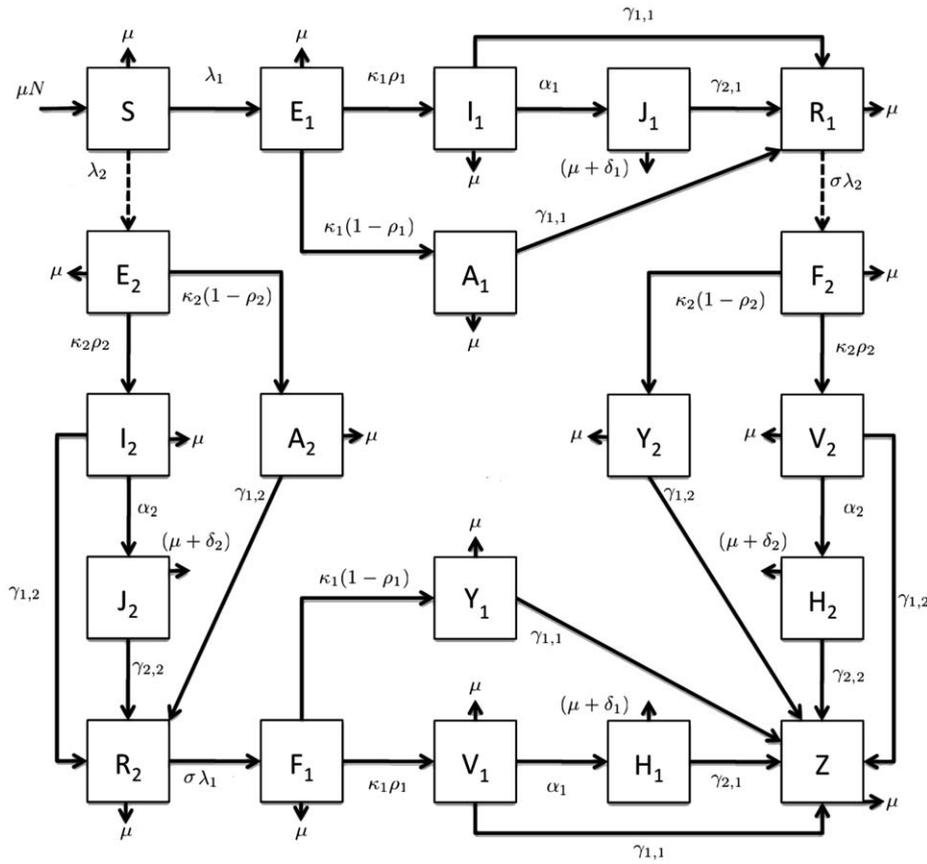
Fig. 1. Flow diagram of the state progression of individuals among the different epidemiological classes as modeled by equations in Appendix A. Individuals can be classified as susceptible (S), exposed (E_i), clinically ill and infectious (I_i), asymptomatic and partially infectious (A_i), diagnosed (J_i), recovered (R_i), exposed to secondary infection (F_i), clinically ill and infectious for secondary infection (V_i), asymptomatic and partially infectious for secondary infection (Y_i), diagnosed for secondary infection (H_i) and recovered to both strains (Z). The solid lines represent the progression between compartments, while the dotted line initializes movement on and after date of the second strain arrival (t_{onset}).
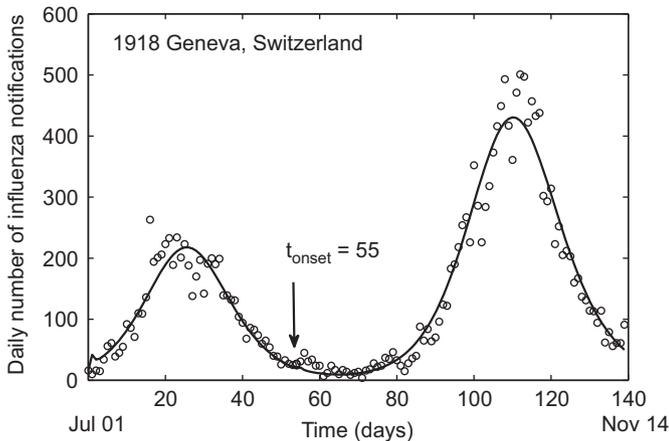

Fig. 2. Our two-strain model fit to the daily number of influenza notifications comprising the spring and fall waves of the 1918 influenza pandemic in Geneva, Switzerland.

our model we used daily epidemic data for Geneva, Switzerland, obtained from mandatory notification registry in Switzerland during the period of July 1918–February 1919 (Ammon, 2002) (Fig. 2). The influenza pandemic affected the Geneva population in two waves, during the summer and fall, respectively. Since the fall wave was reportedly much deadlier than the first, the case fatality proportions (CFP_2) are different for each wave. For Geneva, the first strain CFP_1 was assumed to be 0.7% for the summer wave while CFP was assumed to be 3.25% during the fall wave (Chowell et al., 2006). The total estimated population size of

Geneva, Switzerland, in 1918 was 174,643 (Ammon, 2002), and the average life expectancy was about 60 years. A comprehensive review of the 1918–1919 influenza pandemic in Geneva, Switzerland, is given in Ammon (2001).

We also inspected the pandemic profiles of the 1918 influenza pandemic in several other regions of the world including Gothenburg and Stockholm, Sweden (Andreasen et al., 2008), England and Wales (Chowell et al., 2008a), Copenhagen, Denmark (Kolte et al., 2008), Wroclaw, Poland (Morens and Fauci, 2007), Oslo, Norway (Andreasen et al., 2008), Sydney, Australia (Caley et al., 2007), New York City (Olson et al., 2005) and Newfoundland and Labrador, Canada (Palmer et al., 2007).

2.3. "Arrival" time of a second influenza strain and parameter estimation

We examine the effects of a sequential introduction of the two influenza strains. Guided by the lowest level of influenza incidence observed between waves in the data, the time of arrival of the second strain is considered to occur sometime between day 40 and day 80 after the pandemic onset (Fig. 2). The second epidemic wave is composed of the contribution of all possible infections, i.e. infected by strain 1, infected by strain 1 and then strain 2, and so on. Because the transmission rate and the cross-immunity parameter are not identifiable directly from our data (these parameters multiply each other in the model (Eq. (A.1))), cross-immunity ($1 - \sigma$) is kept fixed at 0.5, a value that is in broad agreement with recent estimates of the level of conferred protection during the 1918–1919 influenza pandemic (Barry et al.,

2008). For each possible value of t_{onset}, we estimate the transmission rate β_1, the recovery rate γ_1, the diagnostic rate α_1, the relative infectiousness of asymptomatic cases q_1, the proportion of clinical cases ρ_1, and the initial numbers of exposed and clinically infectious individuals for the first wave through least squares fitting of the observed cumulative number of notifications, $C(t, \Theta_1)$, in our model (Θ_1 is the vector of estimated parameters for the first wave) to the cumulative number of influenza cases over time, y_t (where t denotes time in days), as described in Chowell et al. (2006). The advantage of using the cumulative over the daily number of new cases is that the former somewhat smoothes out known reporting delays on weekends and national holidays. For the least squares fitting procedure, we used the Levenberg–Marquardt method with line-search implemented in MATLAB (The Mathworks, Inc.) in the built-in routine `lsqcurvefit`, which is part of the optimization toolbox. For simplicity, we only estimate the transmission rate β_2 for the second wave and assume all other parameter estimates to be the same as for the first wave. The best set of parameter estimates is obtained using the χ^2 goodness of fit test statistic.

2.4. The reproduction numbers

The average number of secondary cases generated by a primary infectious case, known as the basic reproduction number R_0 (Anderson and May, 1991; Diekmann and Heesterbeek, 2000), is a measure of the power of an infectious disease to generate an epidemic in a completely susceptible population. In theory, when $R_0 > 1$ an epidemic can occur while an epidemic cannot unfold when $R_0 < 1$. Public health interventions can reduce the value of the basic reproduction number below one in order to prevent an epidemic. For our model in the absence of a second strain, the basic reproduction number is given by (Chowell et al., 2006)

$$R_0 = \frac{\beta_1 \kappa_1}{\kappa_1 + \mu}\left\{\rho_1\left(\frac{1}{\gamma_{1_1} + \alpha_1 + \mu} + \frac{\alpha_1}{(\gamma_{1_1} + \alpha_1 + \mu)(\gamma_{2_1} + \delta_1 + \mu)}\right)\right.$$
$$\left. + (1 - \rho_1)\left(\frac{q_1}{\gamma_{1_1} + \mu}\right)\right\}. \tag{1}$$

The terms comprising the reproduction number can be decomposed into individual contributions from each infectious class (clinical infections, asymptomatic and diagnosed cases). New infections arise at the per capita transmission rate β_1. The fraction of symptomatic cases is given by $\kappa_1 \rho_1 / (\kappa_1 + \mu)$, and the mean time in the infectious class is $1/(\gamma_{1_1} + \alpha_1 + \mu)$. The contribution from the class of diagnosed cases is the product of the fraction of diagnosed symptomatic cases $\kappa_1 \alpha_1 \rho_1 / (\kappa + \mu)(\gamma_{1_1} + \alpha_1 + \mu)$ and the mean infectious period of diagnosed cases which is given by $1/(\gamma_{2_1} + \delta_1 + \mu)$. The contribution from asymptomatic infections is the product of the fraction of asymptomatic cases $\kappa_1(1 - \rho_1)/(\kappa_1 + \mu)$, the relative transmissibility from asymptomatic cases q_1 and the mean time in the asymptomatic class $1/(\gamma_{1_1} + \mu)$.

If the second strain is introduced after the first epidemic wave when the population is no longer completely susceptible, the basic reproduction number alone is no longer relevant to quantify the transmission potential of the second influenza strain. Instead, the factor of interest is the effective reproduction number (R_e) which accounts for the background immunity in the population generated by prior exposure to the first strain in circulation. Here, the effective reproduction number is expressed as

$$R_e = \left(\frac{S(t_{onset}) + \sigma R_1(t_{onset})}{N(t_{onset})}\right)R_{0_2}, \tag{2}$$

where $S(t_{onset})$, $R_1(t_{onset})$ and $N(t_{onset})$ represent the number of susceptible, recovered and total individuals at the time of arrival

of the second strain. The proportion susceptible is dependent on the second strain arrival time and the magnitude of the basic reproduction number of the first strain. The level of protection conferred upon individuals recovered from a first strain infection and the basic reproduction number of the second strain (R_{0_2}) both affect the likelihood of a second strain invading the population. For example, an initial strain with both high levels of transmissibility ($R_{0_1} > 2$) and cross-immunity ($\sigma \ll 1$) will reduce the likelihood of a second outbreak due to the vast number of individuals becoming infected leading to significant effective population immunity levels.

By varying the levels of cross-immunity and the basic reproduction number of the first and second strains we quantify the effective reproduction number (R_e) and identify the critical parameter space where a second strain will not be able to take off ($R_e < 1$). We explore R_0 values in the range of 1–4 which is in agreement with estimates reported for seasonal and pandemic influenza (Chowell and Nishiura, 2008; Chowell et al., 2008b).

3. Results

Using our epidemic model and the time series of influenza notifications for Geneva, Switzerland, during 1918, we estimated model parameters for the first wave of the outbreak, given in Table 1. We further developed a relationship between the level of cross-immunity ($1 - \sigma$) to a variant influenza strain and the basic reproduction number corresponding to each strain (R_{0_1}, R_{0_2}) resulting in an estimate for the effective reproduction number (R_e) for the second wave. We then explored the parameter space for which a secondary wave cannot occur, that is when $R_e < 1$. Furthermore, our model was able to reproduce qualitatively similar historical pandemic profiles of the 1918 influenza pandemic in various regions of the world as we show below.

For the case of Geneva, Switzerland, the initial guess of the second influenza epidemic arrival time (t_{onset}) was on the 72nd day, corresponding to the minimal data point between the summer and fall waves (Fig. 2). The best model fit was obtained when $t_{onset} = 55$ days with a fixed level of cross-immunity between strains ($1 - \sigma = 0.50$) as determined by the χ^2 goodness of fit test statistic. We held this estimated arrival time fixed for further analysis in the context of Geneva, Switzerland. Based on the parameter estimates given in Table 1, the basic reproduction number for the first wave was $R_{0_1} = 1.5$. An increase in the rate of transmission (β_2) for the second strain to fit the model to the second wave resulted in an estimate of $R_{0_2} = 2.4$.

We obtained a theoretical landscape of critical values for R_{0_1} and σ for which one or two waves are possible given the basic reproduction number of the second strain (R_{0_2}) (Fig. 3). Our study reveals that under the presence of cross-immunity, a potential second wave could be prevented. For high levels of R_{0_1} and strong cross-immunity ($\sigma \ll 1$), the likelihood of a secondary wave is significantly diminished. Fig. 3 indicates that a second wave can occur whenever $R_{0_1} < 1.5$ or when cross immunity levels are less than 0.58 ($\sigma > 0.42$) for our estimated R_{0_2} of 2.4.

In Fig. 3, we selected a point (A) in the parameter set (R_{0_1}, σ) within the region where $R_e < 1$ corresponding to $\sigma = 0.10$, $R_{0_1} = 3.0$, which does not support a second wave, and point (B) in the parameter set ($R_{0_1} = 1.5$, $\sigma = 0.35$) corresponds to the two-wave pandemic profile for Geneva, Switzerland, using the second strain reproduction number $R_{0_2} = 2.40$. This relative susceptibility level of $\sigma = 0.35$ can be interpreted as the first wave conferring 65% protection against reinfection during the second wave, which is in line with recent empirical estimates for the 1918 influenza

Table 1
Parameter definitions and baseline estimates for the spring wave of the 1918 influenza pandemic in Geneva, Switzerland.

Parameter	Definition	Source	Spring wave estimate
β_1	Transmission rate (days^{-1})	LS	8.00
$\gamma_{1,1}$	Recovery rate (days^{-1})	LS	0.34
α_1	Diagnostic rate (days^{-1})	LS	0.51
q_1	Relative infectiousness of the asymptomatic class	LS	0.003
ρ_1	Proportion of clinical infections ([0,1])	LS	0.10
$\gamma_{2,1}$	Recovery rate for diagnosed cases (days^{-1})	–	1.10
δ_1	Mortality rate (days^{-1})	Gani et al. (2005)	0.01
κ_1	Rate of progression to infectious (days^{-1})	Mills et al. (2004)	0.53
μ	Birth and natural death rate (days^{-1})	Robine and Paccaud (2005)	$1/(60 * 365)$
$E_1(0)$	Initial number of exposed individuals	LS	207
$I_1(0)$	Initial number of infectious individuals	LS	132

Parameters β_1, γ_1, α_1, q_1, ρ_1, and the initial numbers of exposed and infectious individuals were estimated through least squares (LS) fitting of the model to the cumulative number of influenza notifications as explained in the text. Parameters κ_1 and μ were fixed to baseline estimates obtained from published literature while the mortality rate (δ_1) was estimated from the case fatality proportion as explained in the text. The recovery rate of notified cases is $\gamma_{2_1} = 1/(1/\gamma_{1_1} - 1/\alpha_1)$.
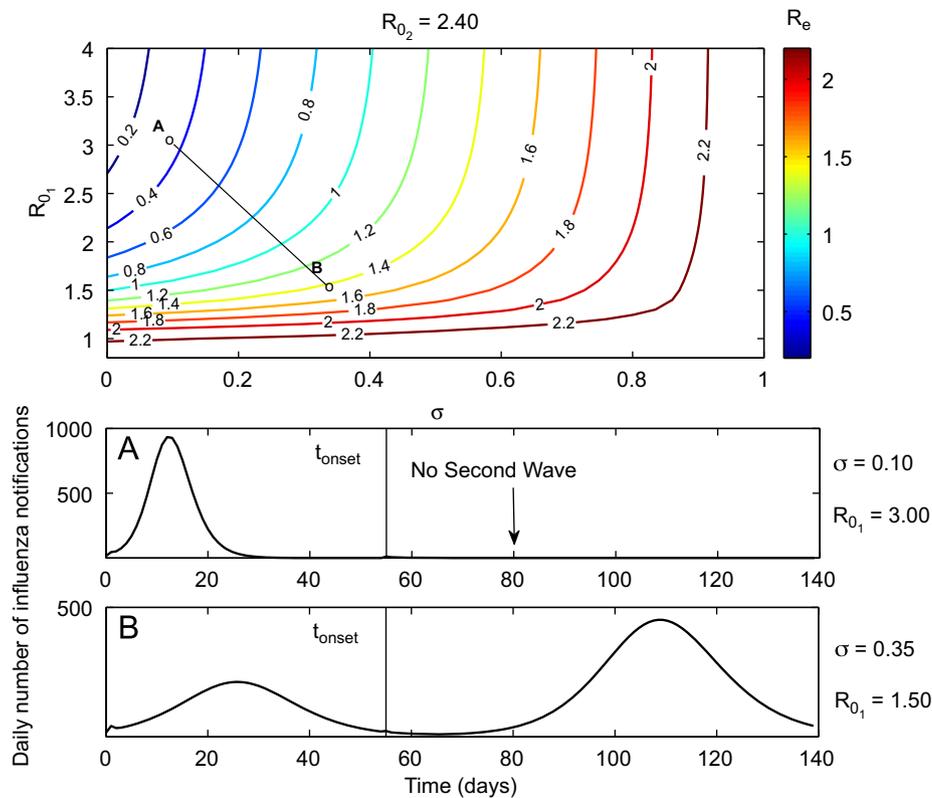

Fig. 3. The effective reproduction number of the second strain varies with the basic reproduction number of the first strain and the level of cross-immunity conferred upon an initial infection. The second strain basic reproduction number is estimated at $R_{0_2} = 2.40$. The contour plot indicates numerical regions for σ and R_{0_1} that will or will not support a second wave. For illustration two points are selected to show the dynamics of our model under different conditions. Point (A) has a level of cross-immunity set at 0.90 ($\sigma = 0.10$), a first strain $R_{0_1} = 3.0$ where $R_e < 1$ (no second wave occurs). Point (B) has a level of cross-immunity of 0.65 ($\sigma = 0.35$), a first strain $R_{0_1} = 1.50$ where $R_e > 1$ (second wave occurs). Point (B) closely resembles the historical profile of the 1918 influenza pandemic in Geneva, Switzerland.

pandemic (Barry et al., 2008). We also extended our analysis by varying the reproduction number of the second strain to explore its impact on the parameter space that supports a second wave (Fig. 4). For this analysis the second strain reproduction number is varied in the range of 1.5–3.0, for illustration. As expected, the parameter space for which a secondary wave is not supported is quickly reduced as the basic reproduction number of the second wave increases.

We identified several pandemic profiles from our review of the time series of cases or deaths of the 1918 influenza pandemic in

several regions (Table 2). For simplicity we classified three main pandemic wave profiles by their shape as: (i) right-handed, (ii) left-handed and (iii) M-shaped. Regions such as Gothenburg and Stockholm, Sweden (Andreasen et al., 2008, Figure 2), Geneva, Switzerland (Ammon, 2002, Figure 2), England and Wales (Chowell et al., 2008a, Figure 1), Copenhagen, Denmark (Kolte et al., 2008, Figure 2), Wroclaw, Poland (Morens and Fauci, 2007, Figure 2A), New York City, USA (Olson et al., 2005, Figure 1), Newfoundland and Labrador, Canada (Palmer et al., 2007, Figure 1) exhibited a right-handed shape wave profile while
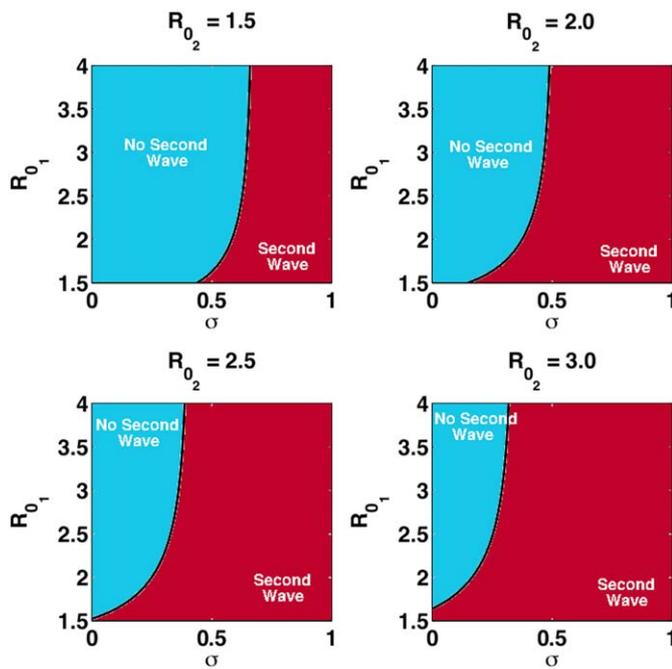
Fig. 4. Critical threshold values for a second pandemic wave for different R_{0_2} values. Levels of cross-immunity and the basic reproduction number of the first wave are simulated. As the second strain's reproduction number increases, the likelihood of a second wave also increases. For instance, when $R_{0_2} = 3.0$, for values of R_{0_1} less than 1.7, the presence of cross-immunity does not prevent a second wave.

Table 2
Regions of the world where several waves of infection have been documented during the 1918–1919 influenza pandemic.

City	Profile type	Source
Geneva, Switzerland	Right hand	Chowell et al. (2006, Figure 2)[b,e]
Gothenburg, Sweden	Right hand	Andreasen et al. (2008, Figure 2)[c]
Stockholm, Sweden	Right hand	Andreasen et al. (2008, Figure 2)[c]
England and Wales	Right hand	Chowell et al. (2008a, Figure 1)[a]
Copenhagen, Denmark	Right hand	Kolte et al. (2008, Figure 2)[c,e]
Wroclaw, Poland	Right hand	Morens and Fauci (2007, Figure 2A)[a]
New York City, US	Right hand	Olson et al. (2005, Figure 1)[d]
Newfoundland and Labrador, Canada	Right hand	Palmer et al. (2007, Figure 2)[a,d]
Oslo, Norway	Left hand	Andreasen et al. (2008, Figure 2)[c]
Sydney, Australia	M-shape	Caley et al. (2007, Figure 2)[b,e]

Pandemic profiles are classified qualitatively as "right hand", "left hand", "M-shape".

[a] Mortality data.
[b] Hospitalization data.
[c] Morbidity incidence data.
[d] Pneumonia and influenza (P and I) mortality data.
[e] See also Fig. 2.

Oslo, Norway (Andreasen et al., 2008, Figure 2) experienced a left-handed wave profile and Sydney, Australia (Caley et al., 2007, Figure 2) resembled the M-shaped profile.

We were able to simulate a number of two-wave pandemic profiles using our mathematical model (Fig. 5). For illustration, the pandemic profiles were scaled to fit in a time frame of 60 days and for all cases the second strain is introduced at time $t_{onset} = 20$

days. When the basic reproduction number of both strains are approximately equal to each other and levels of cross-immunity are low ($\sigma \approx 1$), our model is able to generate the M-shaped profile ($R_{0_1} \approx R_{0_2}$). With a moderately low level of cross-immunity ($\sigma = 0.70$) and a larger first strain basic reproduction number than that of the second strain ($R_{0_1} > R_{0_2}$) our model was able to generate a right-handed wave. Similarly, a left-handed profile was generated by letting the reproduction number of the second strain be larger than that of the first strain ($R_{0_1} < R_{0_2}$) and $\sigma = 0.70$. A trivial concurrent wave case can also be generated by starting both strains at the same time ($t_{onset} = 0$), setting the mean cross-immunity to be 0.50 and the basic reproduction numbers for both strains to be equal to each other ($R_{0_1} = R_{0_2}$).

4. Discussion

We have used a mathematical model that incorporates the interplay between two strains of influenza introduced sequentially in a population to evaluate the impact of the transmissibility associated to each strain, the level of cross-immunity between strains, and the time of introduction of the second strain on the generation of two-wave pandemic profiles of infection that resemble those of the spring/summer and fall waves of the 1918–1919 influenza pandemic. Our mathematical model is an extension to earlier models see Dietz (1979), Castillo-Chavez et al. (1989), Nuño et al. (2005), but to the best of our knowledge, our study is the first in exploring the delayed emergence of a second strain.

Although a number of mechanisms have been shown to generate multiple epidemic waves, and the mechanism or mechanisms responsible for the multiple pandemic profile of the 1918 influenza pandemic still need to be fully clarified, our study is inspired by recent work highlighting the role of cross-immunity in the transmission dynamics of the 1918–1919 influenza pandemic (Barry et al., 2008). Under the assumption that two closely related strains circulated during the 1918 influenza pandemic, our model was able to describe reasonably well the pandemic profile of case notifications in Geneva, Switzerland, and generate a number of qualitative pandemic profiles of the pandemic in other regions of the world by varying the basic reproduction number associated with each strain and levels of cross-immunity. Furthermore, we were able to generate using our model a numerical landscape of critical values of the basic reproduction number of both strains and cross immunity for which a second wave of infection cannot be sustained.

From a public health point of view, our findings indicate that interventions aimed at mitigating the first pandemic wave may be counterproductive by increasing the chances of a second wave of infection that could potentially be more virulent than the first, which was the case for the 1918 influenza pandemic. According to our results, the presence of significant levels of cross-immunity after a highly transmissible first outbreak reduces the likelihood of a second wave. Alternatively, our study suggests that increasing the levels of population immunity through early vaccination campaigns even with a vaccine of limited efficacy could lead to significant levels of population immunity for which a second influenza epidemic may not be able to successfully invade the population. As an analogy, the total number of infected individuals during the first wave can be seen as the total number of individuals naturally "vaccinated" against a closely related variant strain with vaccine efficacy $(1-\sigma)$. For example, Fig. 6 shows the daily number of infections arising from the introduction of two
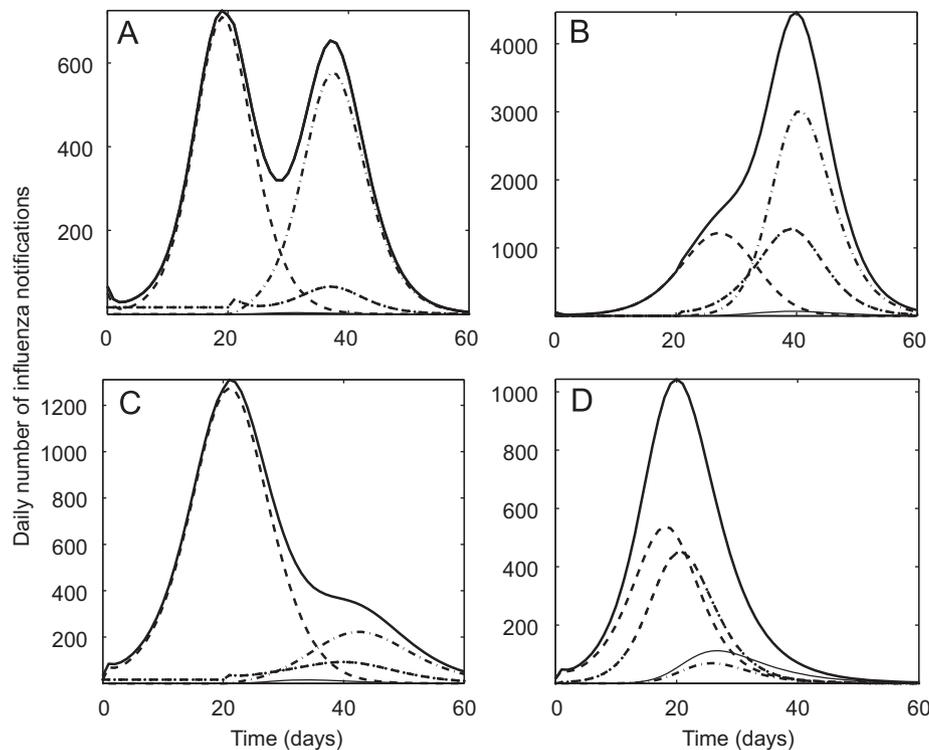
Fig. 5. Four different pandemic profiles generated with our mathematical model by varying the time of introduction (t_{onset}), the level of relative susceptibility to a variant strain (σ) and the reproduction numbers for each strain (R_{0_1}, R_{0_2}). Each subplot ((A), (B), (C), (D)) shows the daily number of influenza notifications over time. Pandemic profiles were classified as follows: (A) M-shape ($t_{onset} = 20, \sigma = 1.0, R_{0_1} \approx R_{0_2}$), (B) right handed wave ($t_{onset} = 20, \sigma = 0.70, R_{0_1} < R_{0_2}$), (C) left handed wave ($t_{onset} = 20, \sigma = 0.70, R_{0_1} > R_{0_2}$) and (D) a concurrent wave ($t_{onset} = 0, \sigma = 0.50, R_{0_1} = R_{0_2}$). The contributions for each pandemic wave are indicated as follows: (solid line (—)) both strains, (dashed line (- -)) strain one, (line with dots (—•)) second strain after being infected with the first, (dashed line with dots (– –•)) strain two, (thin solid line (—)) first strain after being infected with the second.

sequential strains, one at time $t_{onset} = 0$ and the second one at time $t_{onset} = 55$ days. Both basic reproduction numbers are fixed ($R_{0_1} = 2.50$ and $R_{0_2} = 3.75$) and the only parameter varied is the efficacy level of the natural vaccine, thus changing the magnitude and duration of the second wave. A high basic reproduction number for the first strain in circulation implies that the disease is very transmissible, producing a large volume of people in the recovered class after the first wave. The value of $\sigma = 0.30$ is supported by the estimated level of protection conferred by influenza vaccines in healthy adults (70–90%) (Demicheli et al., 2004; Simonsen et al., 2005; Goodwin et al., 2006). In the context of implementing the best control strategy for multiple wave epidemics, see Handel et al. (2007), the parameter set (R_{0_1}, σ) at which the effective reproduction number for the second wave equals one would provide the minimum vaccination coverage and vaccine efficacy necessary to avoid a second wave provided a plausible range of R_{0_2} based on past influenza pandemics (Fig. 3). While Handel et al. (2007) considered a simpler setting with the same infectious agent for epidemic waves (with the same R_0), we have considered a scenario of two strains of influenza related via cross-immunity and connected our framework to time series data of the 1918 influenza pandemic. In the context of pandemic preparedness, our results indicate that avoiding a second influenza pandemic wave is plausible given sufficient levels of protection are attained via natural infection and/or vaccination campaigns during an early wave of infection. We note that our threshold results are conservative because we did not account for control interventions such as social distancing and, isolation of infectious individuals.

Our results highlight the importance of generating reliable estimates of the attack rate of an initial "herald" influenza pandemic wave characteristic of influenza pandemics (Miller et al., 2009) to generate bounds on the vaccination coverage that would be necessary to contain a second wave using information on the transmissibility of past pandemics and a plausible range of cross-immunity levels. For the initial pandemic wave of the novel swine-origin A(H1N1) influenza virus having Mexico as the epicenter and currently circulating around the world, early estimates of R_{0_1} in the range of 1.4–3.0 (Boëlle et al., 2009; Fraser et al., 2009; Nishiura et al., 2009) together with planned vaccination campaigns with plausible national coverage levels in the range of 5–30% prior to a possible second fall/winter wave highlight the possibility of achieving sufficient levels of background immunity in the population that could avert or at least mitigate a potential second pandemic wave.

Appendix A. Model equations

The transmission dynamics of two strains of influenza can be modeled using the following system of nonlinear differential equations, where $i \in [1, 2], i \neq j$. Parameter definitions and values
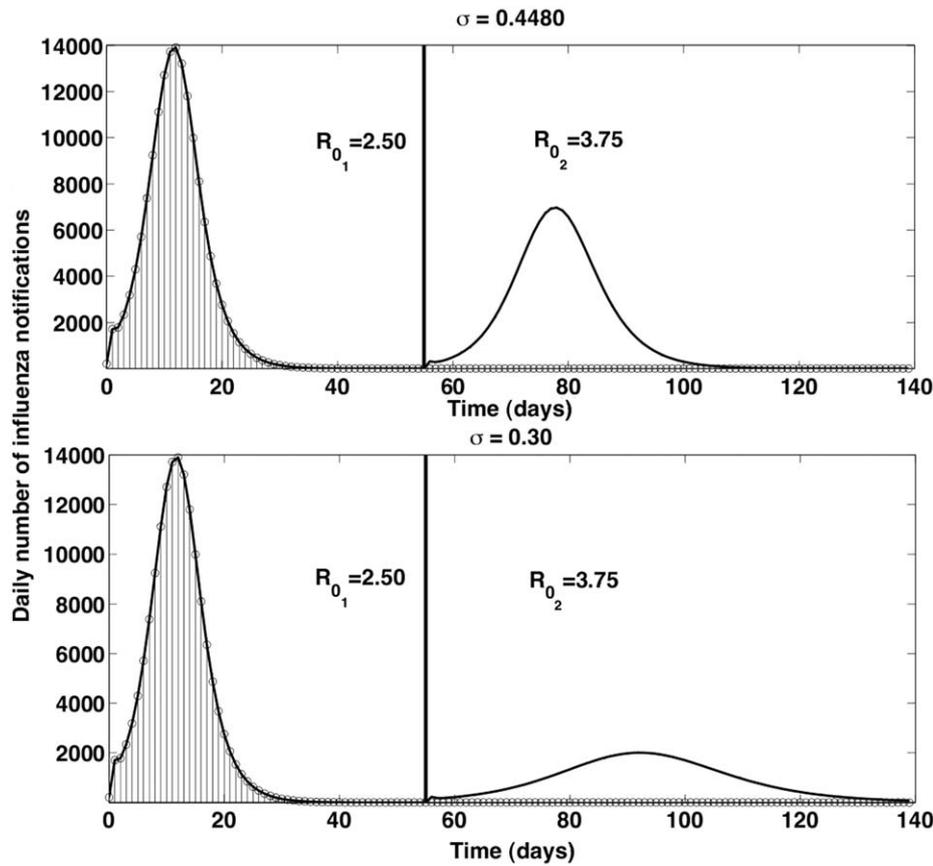
Fig. 6. The total number of individuals infected during the first wave can be seen as the total number of individuals naturally "vaccinated" against a variant strain with efficacy $1 - \sigma$ (shaded region). The daily number of infections arising from the second strain at $t_{onset} = 55$ is shown for two different levels of relative susceptibility to the second strain ($\sigma = 0.4489$ and 0.30) when $R_{0_1} = 2.50$ and $R_{0_2} = 3.75$.

are given in Table 1.

$$
\begin{cases}
\dot{S}(t) = \mu N(t) - (\lambda_1(t) + \lambda_2(t) + \mu)S(t), \\
\dot{E}_i(t) = \lambda_i(t)S - (k_i + \mu)E_i, \\
\dot{A}_i(t) = k_i(1 - \rho_i)E_i - (\gamma_{1_i} + \mu)A_i, \\
\dot{I}_i(t) = k_i\rho_i E_i - (\alpha_i + \gamma_{1_i} + \mu)I_i, \\
\dot{J}_i(t) = \alpha_i I_i - (\gamma_{2_i} + \delta_i + \mu)J_i, \\
\dot{R}_i(t) = \gamma_{1_i}(A_i + I_i) + \gamma_{2_i}J_i - (\sigma\lambda_j(t) + \mu)R_i, \quad i \neq j, \\
\dot{F}_i(t) = \sigma\lambda_j(t)R_i - (k_i + \mu)F_i, \quad i \neq j, \\
\dot{Y}_i(t) = k_i(1 - \rho_i)F_i - (\gamma_{1_i} + \mu)Y_i, \\
\dot{V}_i(t) = k_i\rho_i F_i - (\alpha_i + \gamma_{1_i} + \mu)V_i, \\
\dot{H}_i(t) = \alpha_i V_i - (\gamma_{2_i} + \delta_i + \mu)H_i, \\
\dot{Z}(t) = \displaystyle\sum_{i=1}^{2}(\gamma_{1_i}(Y_i + V_i) + \gamma_{2_i}H_i) - \mu Z, \\
\dot{C}(t) = \displaystyle\sum_{i=1}^{2}(\alpha_i(I_i + V_i)),
\end{cases}
\tag{A.1}
$$

where $\lambda_i(t) = \beta_i(I_i(t) + J_i(t) + q_i A_i(t) + V_i(t) + H_i(t) + q_i Y_i(t))/N(t)$.

References

Ammon, C., 2001. The 1918 Spanish flu epidemic in Geneva, Switzerland. In: International Congress Series, vol. 1219, pp. 163–168.

Ammon, C., 2002. Spanish flu epidemic in 1918 in Geneva, Switzerland. Euro Surveill. 7, 190–192.

Anderson, R., May, R., 1991. Infectious Diseases of Humans. Oxford University Press, New York.

Andreasen, V., Viboud, C., Simonsen, L., 2008. Epidemiological characterization of the 1918 influenza pandemic summer wave in Copenhagen: implications for pandemic control strategies. J. Infect. Dis. 197, 270–278.

Barry, J., Viboud, C., Simonsen, L., 2008. Cross-protection between successive waves of the 1918–1919 influenza pandemic: epidemiological evidence from US Army camps and from Britain. J. Infect. Dis. 198 (10), 1427–1435.

Boëlle, P., Bernillon, P., Desenclos, J., 2009. A preliminary estimation of the reproduction ratio for the new influenza A(H1N1) from the outbreak in Mexico, March–April 2009. Euro Surveill. 14 (19), 19205.

Caley, P., Philip, D., McCracken, K., 2007. Quantifying social distancing arising from pandemic influenza. J. R. Soc. Interface 5 (23), 631–639.

Castillo-Chavez, C., Hethcote, H., Andreasen, V., Levin, S., Liu, W., 1989. Epidemiological models with age structure, proportionate mixing, and cross immunity. J. Math. Biol. 27, 233–258.

Chowell, G., Ammon, C., Hengartner, N., Hyman, J., 2006. Transmission dynamics of the great influenza pandemic of 1918 in Geneva, Switzerland: assessing the effects of hypothetical interventions. J. Theor. Biol. 241 (2), 193–204.

Chowell, G., Bettencourt, L., Johnson, N., Alonso, W., Viboud, C., 2008a. The 1918–1919 influenza pandemic in England and Wales: spatial patterns in transmissibility and mortality impact. Proc. R. Soc. B 275, 501–509.

Chowell, G., Miller, M., Viboud, C., 2008b. Seasonal influenza in the United States France and Australia: transmission and prospects for control. Epidemiol. Infect. 136, 852–864.

Chowell, G., Nishiura, N., 2008. Quantifying the transmission potential of pandemic influenza. Phys. Life Rev. 5, 50–77.

Demicheli, V., Rivetti, D., Deeks, J., Jefferson, T., 2004. Vaccines for preventing influenza in healthy adults. Cochrane Database Syst. Rev. 3, CD001269.

Diekmann, O., Heesterbeek, J., 2000. Mathematical Epidemiology of Infectious Diseases: Model Building, Analysis and Interpretation. Wiley, New York.

Dietz, K., 1979. Epidemiologic interference of virus populations. J. Math. Biol. 8, 291–300.

Epstein, J., Parker, J., Cummings, D., Hammond, R., 2008. Coupled contagion dynamics of fear and disease: mathematical and computational explorations. PLoS One 3 (12), e3955.

Fox, J., Hall, C., Cooney, M., Foy, H., 1982. Influenza viruses infections in Seattle families 1975–1979. Am. J. Epidemiol. 116, 212–227.

Fraser, C., Donnelly, C., Cauchemez, S., Hanage, W., Van Kerkhove, M., et al., 2009. Pandemic potential of a strain of influenza A (H1N1): early findings. Science 324 (5934), 1557.

Gani, R., Hughes, H., Fleming, D., Grifin, T., Medlock, J., Leach, S., 2005. Potential impact of antiviral use during influenza pandemic. Emerg. Infect. Dis. 11, 1355–1365.

Goodwin, K., Viboud, C., Simonsen, L., 2006. Antibody response to influenza vaccination in the elderly: a quantitative review. Vaccine 24 (8), 1159–1169.

Handel, A., Longini, I., Antia, R., 2007. What is the best control strategy for multiple infectious disease outbreaks?. Proc. Biol. Sci. 274 (1611), 833–837.

Kolte, I., Skinhoj, P., Keiding, N., Lynge, E., 2008. The Spanish flu in Denmark. Scand. J. Infect. Dis. 40, 538–546.

Merler, S., Poletti, P., Ajelli, M., Caprile, B., Manfredi, P., 2008. Coinfection can trigger multiple pandemic waves. J. Theor. Biol. 254 (2), 499–507.

Mexico Ministry of Health, 2009. Update on the S-OIV epidemic in Mexico, July. Available online ⟨http://portal.salud.gob.mx/contenidos/noticias/influenza/estadisticas.html⟩.

Miller, M., Viboud, C., Balinska, M., Simonsen, L., 2009. The signature features of influenza pandemics—implications for policy. N. Engl. J. Med. 360 (25), 2595–2598.

Mills, C., Robine, J., Lipsitch, M., 2004. Transmissibility of 1918 pandemic influenza. Nature 432 (7019), 904–906.

Morens, D., Fauci, A., 2007. The 1918 influenza pandemic: insights for the 21st century. J. Infect. Dis. 195, 1018–1028.

Nishiura, H., Castillo-Chavez, C., Safan, M., Chowell, G., 2009. Transmission potential of the new influenza A(H1N1) virus and its age-specificity in Japan. Euro Surveill. 14 (22), 19227.

Nuño, M., Feng, Z., Martcheva, M., Castillo-Chavez, C., 2005. Dynamics of two-strain influenza with isolation and partial cross-immunity. SIAM J. Appl. Math. 65 (3), 964–984.

Olson, D., Simonsen, L., Edelson, P., Morse, S., 2005. Epidemiological evidence of an early wave of the 1918 influenza pandemic in New York City. Proc. Natl. Acad. Sci. USA 102 (31), 11059–11063.

Palmer, C., Sattenspiel, L., Cassidy, C., 2007. The spread of the Spanish flu on the island of Newfoundland. Newfoundland and Labrador Stud. 22, 1719–1726.

Patterson, K., Pyle, G., 1991. The geography and mortality of the 1918 influenza pandemic. Bull. Hist. Med. 65, 4–21.

Robine, J., Paccaud, F., 2005. Nonagenarians and centenarians in Switzerland, 1860–2001: a demographic analysis. J. Epidemiol. Community Health 59 (1), 31–37.

Simonsen, L., Reichert, T., Viboud, C., Blackwelder, W., Taylor, R., Miller, M., 2005. Impact of influenza vaccination on seasonal mortality in the US elderly population. Arch. Intern. Med. 165 (3), 265–272.

Taber, L., Paredes, A., Glezen, W., Couch, R., 1981. Infection with influenza A/Victoria virus in Houston families 1976. J. Hyg. (Lond) 86, 303–313.